Copy No.

RM No. L8H06

NACA

RESEARCH MEMORANDUM

PRESSURE DISTRIBUTIONS OVER A WING-FUSELAGE MODEL AT MACH NUMBERS OF 0.4 TO 0.99 AND AT 1.2

By

Clarence W. Matthews

Langley Aeronautical Laboratory
Langley Field, Va.

NATIONAL ADVISORY COMMITTEE FOR AERONAUTICS

WASHINGTON

November 3, 1948

NACA RM No. L8H06

NATIONAL ADVISORY COMMITTEE FOR AERONAUTICS

RESEARCH MEMORANDUM

PRESSURE DISTRIBUTIONS OVER A WING-FUSELAGE MODEL AT MACH NUMBERS OF 0.4 TO 0.99 AND AT 1.2

By Clarence W. Matthews

SUMMARY

Pressure distributions over a prolate spheroid of fineness ratio 6 and about a combination of this body with an NACA 65-010 wing section have been obtained at Mach numbers of 0.4 through 0.99 and at 1.2 in the Langley 8-foot high-speed tunnel. For these tests the ratio of model cross section to tunnel cross section was very small.

The transition from a subsonic to a supersonic flow pattern occurred in a continuous manner within the Mach number range between the critical Mach number and a Mach number slightly below unity. The pressure distributions change in this region in such a manner as to indicate a greatly increasing drag. The application of an extension of the Prandtl-Glauert method for subcritical axially symmetric flow was found to approximate the compressibility effect, particularly near the midsection of the body; extrapolation into the supercritical region showed increasing departure from the experiment. The tunnel-wall interference was found to be negligible even at the choking Mach number.

INTRODUCTION

Because the ratios of model cross section to tunnel cross section usually existing in high-speed-tunnel testing are such that the tunnel is choked at some stream Mach number below 0.95, there are very little wind-tunnel data available concerning the aerodynamic characteristics of flow between stream Mach numbers of 0.95 and 1.20. In conjunction with another project, tests were made in the Langley 8-foot high-speed tunnel on a small model between Mach numbers of 0.4 and 0.99 and at 1.2. The results of these tests are analyzed in this paper to show the general nature of the flow in this Mach number range. The tests consisted of pressure measurements over a prolate spheroid and about a model consisting of the same body plus a wing. The experimental subcritical results of the flow over the prolate spheroid are compared with theoretically calculated results.

MODEL

A sketch of the model used in the tests is shown in figure 1. The body of the model was a prolate spheroid with a fineness ratio of 6. The wing was an NACA 65-010 airfoil section with a total span of 6 inches and an aspect ratio of 4; it was placed in the midwing position with its chord direction coinciding with the axis of the prolate spheroid. Pressure orifices were located over the top of the body with several check orifices located diametrically opposite on the bottom. The wing pressure orifices were located on the top of the wing. The chordwise orifices were halfway between the root and tip of the wing, and those in the spanwise direction were distributed along the 50-percent-chord line. Two pressure orifices were located on the bottom of the wing. The model was supported in the tunnel with a $\frac{1}{2}$-inch-diameter sting which was connected to the body as shown in figure 1. The angle-of-attack coupling was located in the sting 10 inches away from the model.

Tests.- The tests were made in the Langley 8-foot high-speed tunnel equipped with a 1.2 Mach number supersonic nozzle. The subsonic tests were made in the throat of the supersonic nozzle. The supersonic tests were made in the best portion of the supersonic nozzle. In either case, the variations in Mach number over the test region employed were not over ± 0.005.

The subsonic stream Mach number was determined from empty-tunnel calibrations. Three separate calibration orifices, located in the tunnel wall 16, 28, and 44 inches upstream of the model, were used. The variation in the stream Mach numbers indicated by the orifices was 0.002.

The model was tested at 0° angle of attack both with and without the wing and at 10° angle of attack with the wing.

RESULTS

The Mach number and pressure-coefficient distributions were calculated from the pressure data taken over the model and are presented as functions of body length, span length, and chord length in figures 2 to 15. These figures show the development of flow from subsonic through the supercritical range up to a Mach number of 0.99 and at a Mach number of 1.2. The Mach numbers were calculated from the total-head values with no correction for shock losses; however, at a stream Mach number $M_s = 1.2$ the losses even for a normal shock were small so that the errors were negligible

The Reynolds number per foot of the flow over the model varied between 2,690,000 at $M_s = 0.4$ and 3,960,000 at $M_s = 0.99$ and was 3,820,000 at $M_s = 1.2$.

Wall and sting interference.- Since the ratio of model cross section to tunnel cross section is only 0.00032, the wall interference may be expected to be very small. The theoretical wall-interference corrections, given by extrapolating to supercritical Mach numbers the results of references 1 and 2, indicate that the Mach number correction factor for an indicated stream Mach number of 0.98 is 1.0032 for the body and wing at 0° angle of attack. The corrections for pressure coefficient, Reynolds number, and drag are correspondingly small.

The experimental Mach number distributions at the wall (fig. 16) show only a negligible effect of the model, less in fact than the day-to-day variation in the calibration. Since according to reference 2 the interference velocities (to which the induced Mach numbers are proportional) are only 0.454 times the induced velocities at the wall, it therefore follows that the interference velocities (or Mach numbers) must also be negligible. It may be noted from figure 16 that the difference between the wall Mach numbers with and without the model present increases considerably in the region downstream from the model. This effect is to be expected because of the large increase in cross section of the sting support in this region.

The experimentally obtained choking Mach number of 0.99 exceeded the theoretical value of 0.98. The excess may possibly be due to boundary-layer thinning as discussed in reference 3.

Another type of interference may be seen by examining the subcritical pressure distributions of figure 3. Although the body is symmetrical about its center, the pressures are more positive over the rear of the body than over the forward part. This is obviously an effect caused by the sting, since viscosity and tunnel-wall-interference effects tend to prevent pressure recovery. This sting-interference effect exists as far forward as the 40- to 50-percent station on the body. Except for a possible reaction through the boundary layer, no such interference is to be expected with supersonic speeds.

ANALYSIS

Nature of flow over a model in transonic region.- A number of tests on bodies of revolution by the wing-flow method (reference 4) have shown an asymmetrical pressure distribution for stream Mach numbers near unity

in which the peak negative pressure coefficients shifted rearward once the critical velocity was attained. An examination of figures 3, 5, and 11 shows that this phenomenon also occurs in the present wind-tunnel tests. Figures 5 and 11 show though that the presence of the wing restricts the rearward movement of the negative pressure peak. The chordwise pressure distributions over the center of the wing (figs. 7 and 13) also show the same rearward movement of the pressure peak as the critical Mach number is attained. This shift of pressure coefficients which occurs on all the component parts of the model after the critical velocity has been reached indicates that a very marked increase in drag may be expected at Mach numbers just below unity. This shift is to be expected because of the velocity increases due to the local supersonic-flow expansion which occurs over the rear of the body.

Development of supersonic flow from subsonic flow.- Examination of the Mach numbers over a prolate spheroid, figure 2, shows no marked change in the shape of the Mach number distribution curve until local supersonic flow is attained on the body. Then, as previously discussed, the peak Mach numbers continuously move rearward. The shape of the distribution near the nose also changes. However, as in the case of the rearward movement of the peak Mach number, this change is also gradual. Thus, these results indicate that the supersonic-flow pattern develops continuously from the subsonic pattern as the stream Mach number progresses through the supercritical region.

Adding a wing to the body (figs. 4 and 10) does not materially change the continuity of the development of transonic flow from the subsonic condition. The changes in local Mach number over the body when the wing is installed increase more rapidly with increasing Mach number than do those changes with the body alone, indicating that compressibility effects at high subsonic Mach numbers are relieved by three-dimensional flow.

Similar trends in continuity and rearward movement of Mach number peaks may also be noted in the chordwise distributions over the center of the wing at both 0° and 10° angle of attack (figs. 6 and 12). At 0° angle of attack, the curves are quite regular and have the same shape so long as the flow is subcritical. After a local supersonic flow has been attained on the wing, the Mach number peak moves rearward, thereby developing the supersonic-flow pattern at $M_s = 0.98$. The shape of the distribution is not materially changed when the stream Mach number is increased from 0.98 to 1.2. The distributions for 10° angle of attack (fig. 12) present more complicated changes after the flow becomes critical. The step-like change which occurs between $M_s = 0.766$ and $M_s = 0.938$ may be due to an oblique shock followed by separation. Above $M_s = 0.938$ the distribution flattens out, indicating that the

[redacted]

flow separates at the highest point on the wing. This condition exists up to a stream Mach number of 0.99. The change of the shape of the distribution when the stream Mach number increases to 1.2 indicates that the flow becomes reattached to the airfoil. It thus appears that the supersonic flow tends to reduce separation.

The changes in the shape of the chordwise pressure distributions over the top of the airfoil indicate important shifts in the location of the center of pressure of the airfoil. The subcritical curves are essentially similar in shape so that there will be very little shift in the center of pressure until critical velocities appear on the airfoil. Once the critical velocity has been attained, the center of pressure starts moving rearward with increasing Mach number and attains its approximate final position at $M_s = 0.97$ to 1.00.

The spanwise Mach number and pressure distributions (figs. 8, 9, 14, and 15) are difficult to interpret because of the lack of pressure data; that is, it is not known whether the changes are due to general increases in the chordwise distributions or to changes in the locations of the peak values. However, at 0° angle of attack, the subcritical Mach numbers and pressure coefficients are relatively constant along the center of the wing. Then, as supercritical flow develops, a step-like increase in Mach numbers and negative pressure coefficients starts at the wing root and with increasing Mach number moves out to the tip of the wing. The curves then level off for stream Mach numbers near 1 and at 1.2. This step-like increase indicates that a supersonic region first forms near the body and then moves out toward the tip of the wing with increasing stream Mach number. The curves at 10° angle of attack are extremely complicated by separation phenomena. It is to be noted though that the $M_s = 1.2$ curves have the same shape as those at $M_s = 0.99$. If the spanwise pressure coefficients (fig. 15) are an indication of the lift distribution over the airfoil, the lift at subsonic speeds is definitely inboard; at supercritical speeds it moves outboard, and then becomes more or less evenly distributed at low supersonic speeds.

These tests indicate that the transition from a subsonic- to a supersonic-flow pattern starts shortly after the flow over the body becomes critical, and that the transition is complete, except over the rearmost part of the body, by the time the stream Mach number becomes 0.97 or thereabouts. A possible explanation for the fact that the supersonic-flow pattern develops at subsonic stream Mach numbers is that because of the induced velocities due to the model the velocity field about the model at a stream Mach number of 0.97 or 0.98 is already largely supersonic so that the model appears to be in a supersonic field; hence, it may be expected that the flow over the body will exhibit supersonic characteristics at stream Mach numbers just below 1.

[redacted]

Comparison of experimental and theoretical flow at subsonic stream Mach numbers.- The theoretical values of the pressure coefficients over a prolate spheroid of fineness ratio 6 were calculated. Compressibility effects were included by using the modification of the Prandtl-Glauert method suggested in reference 5. The calculated values are compared with the experimental values in figure 17. These curves show that, for subcritical flow, the compressibility corrections given in reference 5 result in fair agreement rearward of the 5-percent station. When the flow becomes critical though, the errors tend to become greater farther back on the body, but are still reasonably small near the midsection of the body. Once the supersonic-flow pattern develops, that is at stream Mach numbers of 0.97 and higher, the method becomes inapplicable.

These results indicate that the Prandtl-Glauert method may be applied to subsonic flow with a fair degree of approximation, and that it may be extrapolated slightly into the supercritical region, with the expectation that the resultant error will be greater the more the critical stream Mach number is exceeded.

CONCLUSIONS

For the wing-fuselage body investigated, the following conclusions were made:

1. The asymmetrical supersonic-flow pattern develops continuously from the subsonic-flow pattern. The development starts at a stream Mach number slightly above critical and is complete except at the rearmost part of the body at a stream Mach number of 0.96 or 0.97.

2. The drag increase, which has been observed at Mach numbers between 0.93 and 1.00, is due to an increase in the pressure drag caused by the rearward movement of the negative pressure peaks which is the result of the development of the supersonic-flow pattern before a stream Mach number of 1 is attained.

3. As the ratio of model-to-tunnel cross section is decreased, the maximum stream Mach number at which the results are not invalidated by wall interference becomes very nearly equal to the choking Mach number.

4. The extension of the Prandtl-Glauert method to axially symmetric flow may be applied to subsonic flow with a fair degree of approximation,

and extrapolated slightly into the supercritical region, with the expectation that the resultant error will be greater the more the critical Mach number is exceeded.

Langley Aeronautical Laboratory
National Advisory Committee for Aeronautics
Langley Field, Va.

REFERENCES

1. Herriot, John G.: Blockage Corrections for Three-Dimensional-Flow Closed-Throat Wind Tunnels, with Consideration of the Effect of Compressibility. NACA RM No. A7B28, 1947.

2. Baranoff, A. v.: Tunnel Correction for Compressible Subsonic Flow. NACA TM No. 1162, 1947.

3. Matthews, Clarence W., and Wright, Ray H.: Investigation of Flow Conditions and the Nature of the Wall-Constriction Effect near and at Choking by Means of the Hydraulic Analogy. NACA RM No. L8F17, 1948.

4. Danforth, Edward C. B., and Johnston, J. Ford.: Pressure Distribution over a Sharp-Nose Body of Revolution at Transonic Speeds by the NACA Wing-Flow Method. NACA RM No. L7K12, 1948.

5. Hess, Robert V., and Gardner, Clifford S.: Study by the Prandtl-Glauert Method of Compressibility Effects and Critical Mach Number for Ellipsoids of Various Aspect Ratios and Thickness Ratios. NACA RM No. L7B03a, 1947.

[redacted]

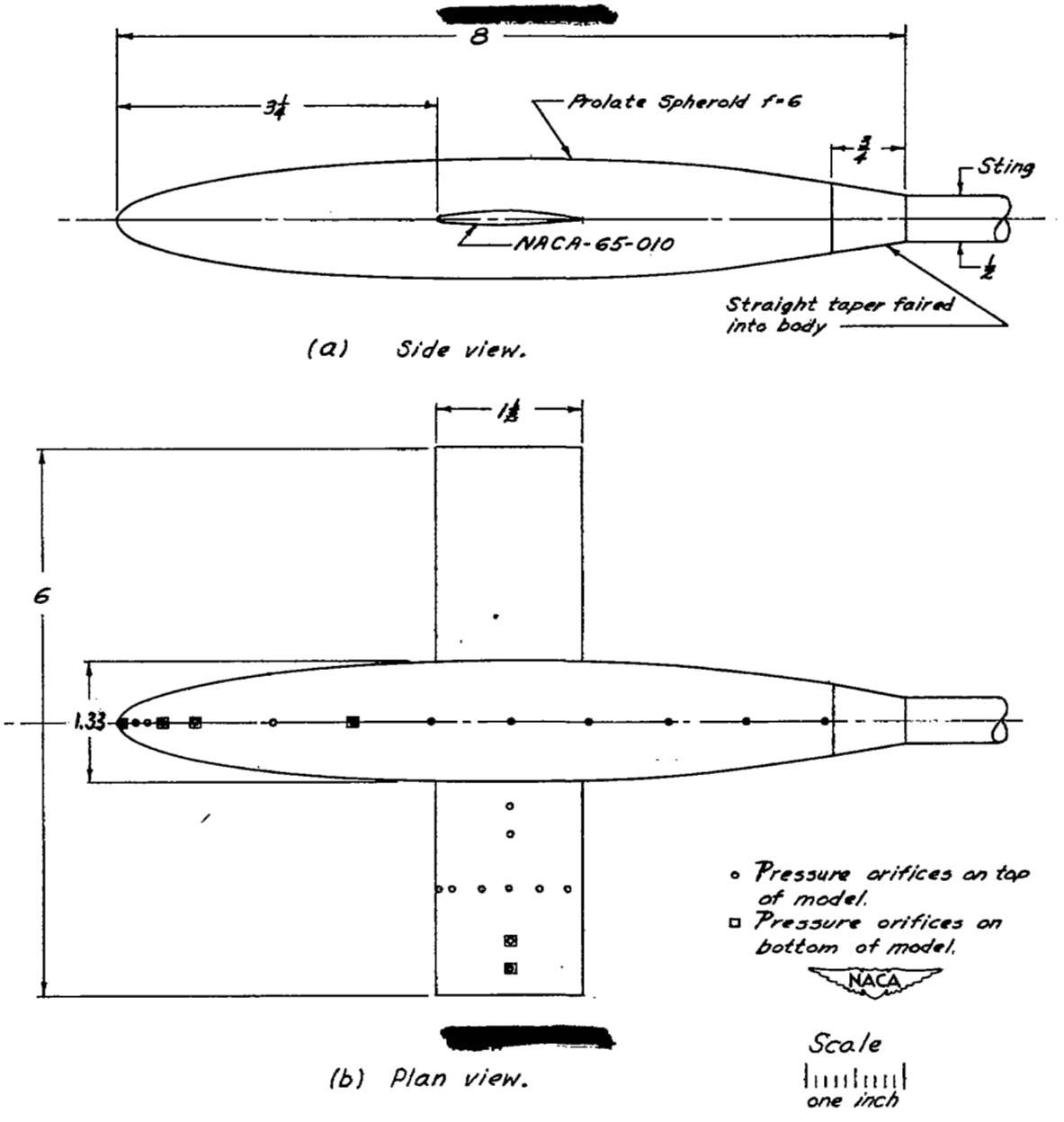

Figure-1 Schematic view of complete model.
(All dimensions in inches.)

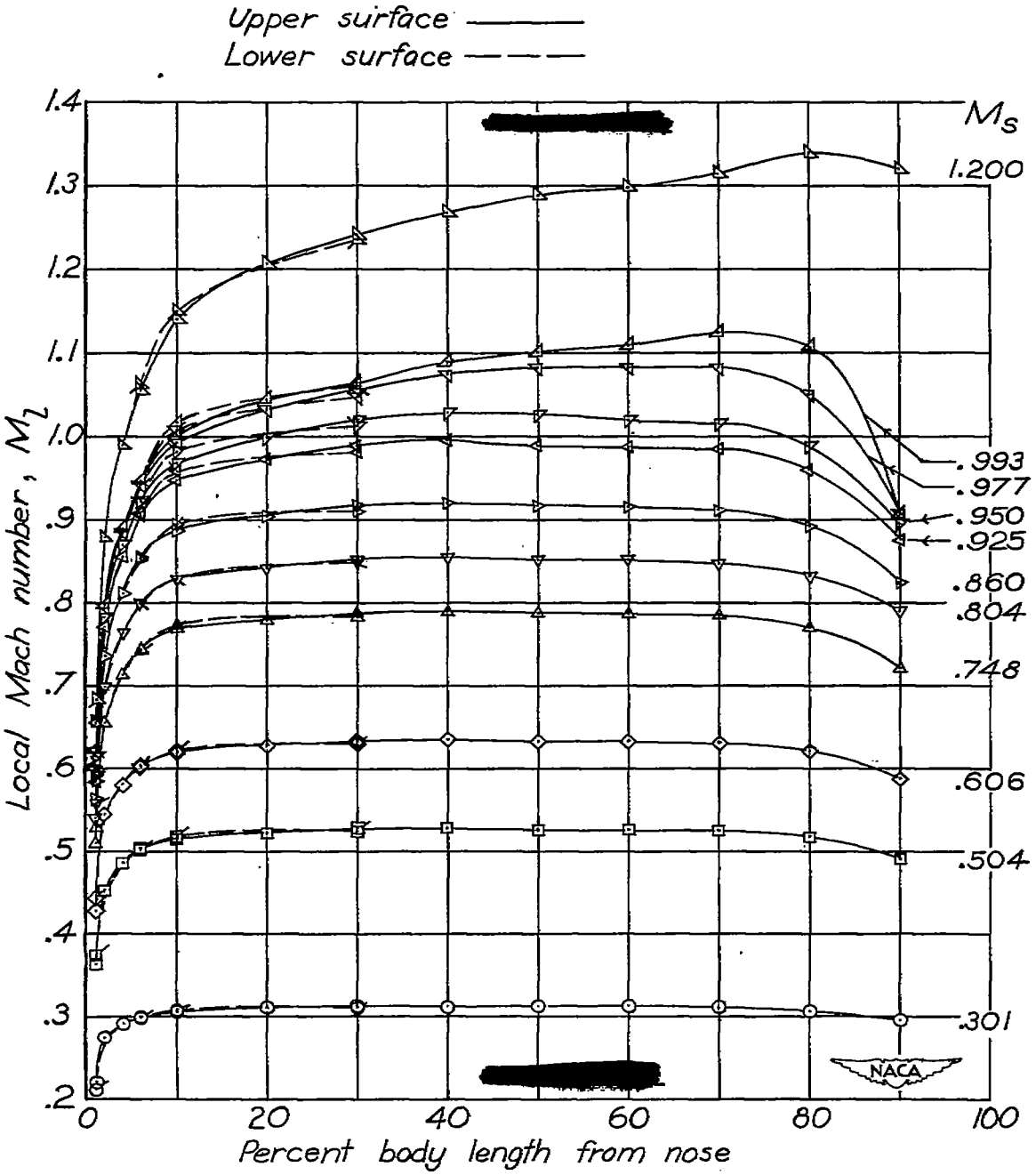

Figure 2.— Mach number distribution about a prolate spheroid of fineness ratio 6 for various stream Mach numbers. $\alpha = 0°$. (The plain symbols refer to the upper surface and the flagged symbols refer to the lower surface.)

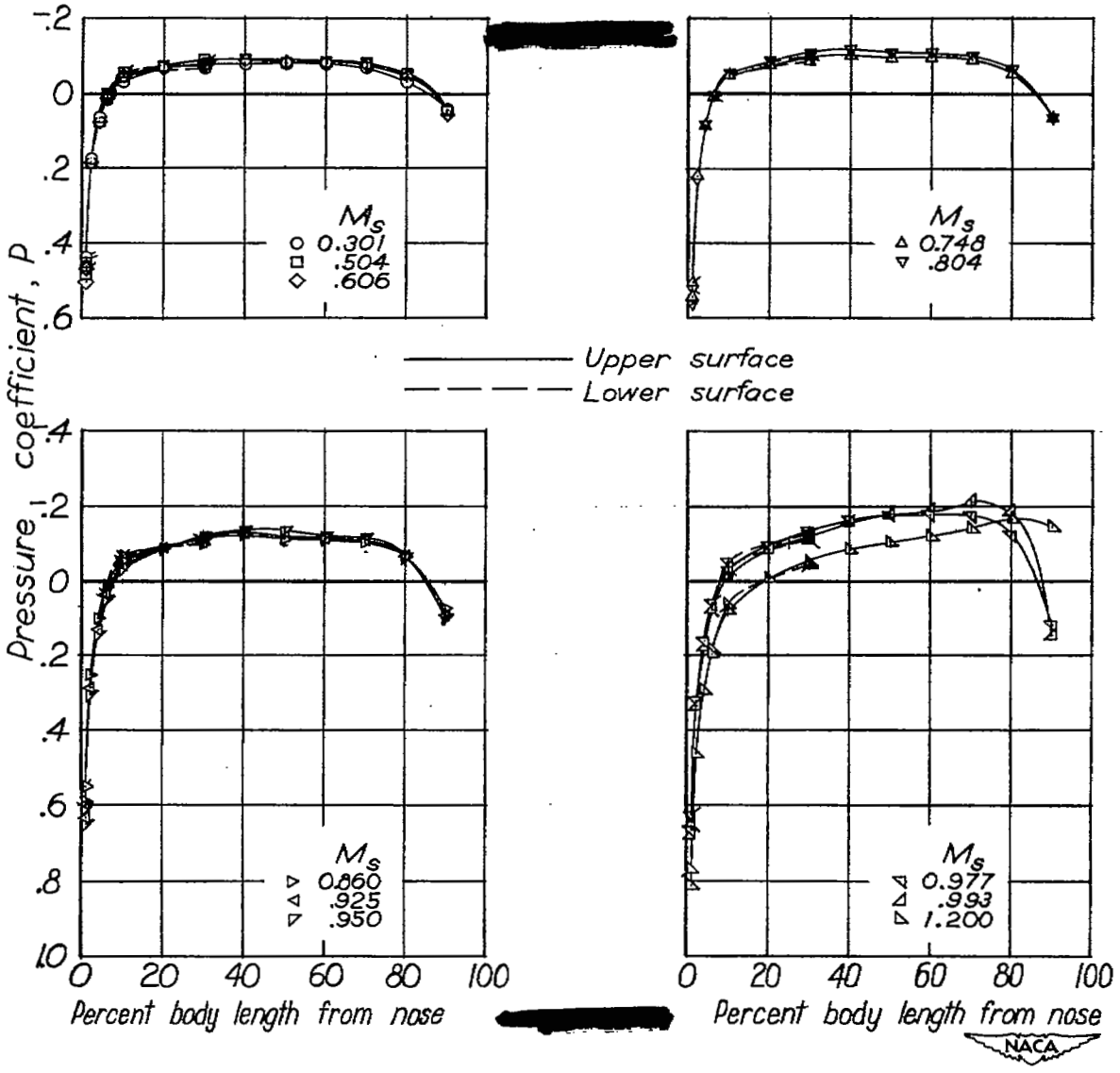

Figure 3.— Pressure distribution about a prolate spheroid with fineness ratio 6 for various stream Mach numbers. $\alpha = 0°$. (The plain symbols refer to the upper surface and the flagged symbols refer to the lower surface.)

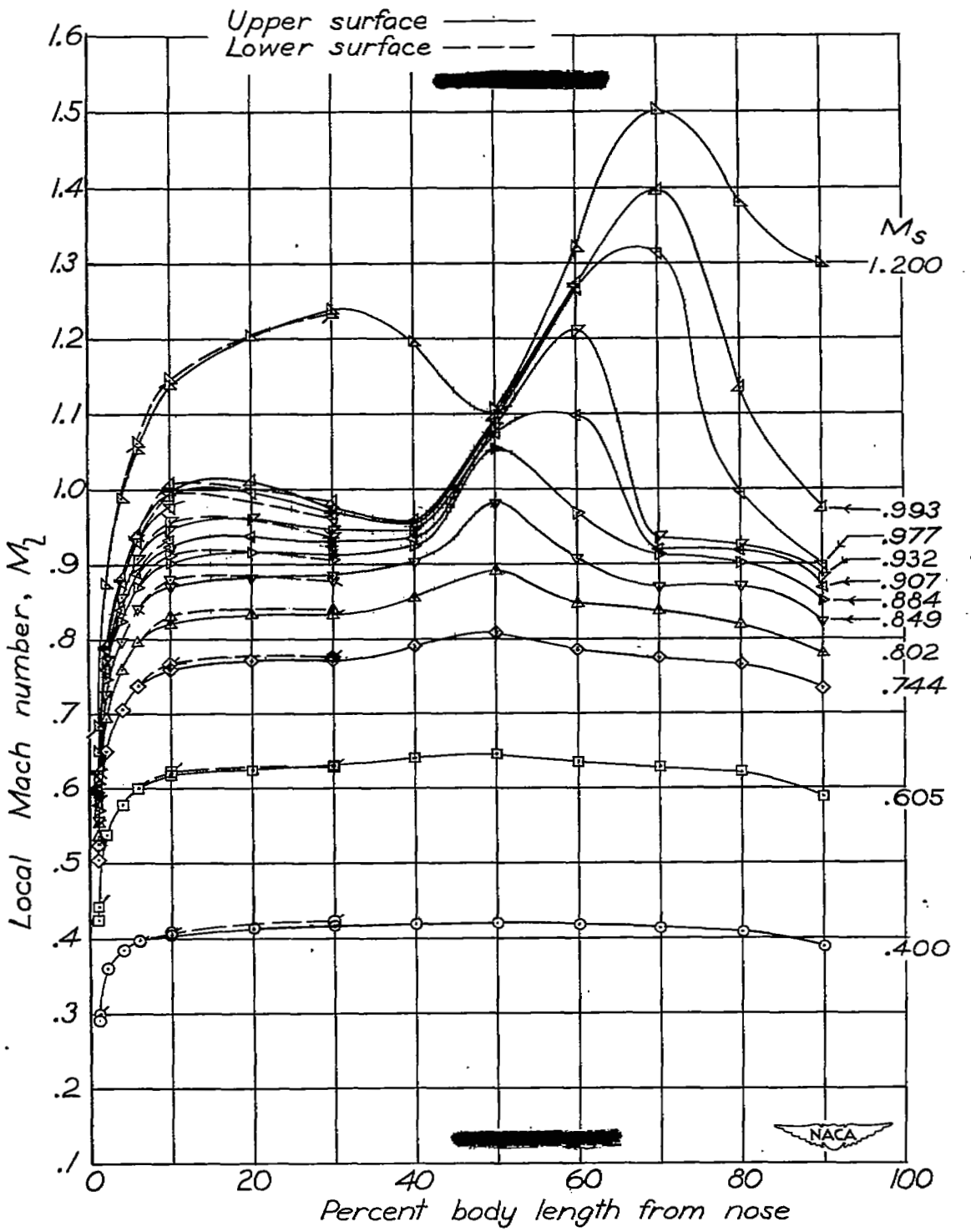

Figure 4.— Mach number distribution about fuselage. Complete model; $\alpha = 0°$. (The plain symbols refer to the upper surface and the flagged symbols refer to the lower surface.)

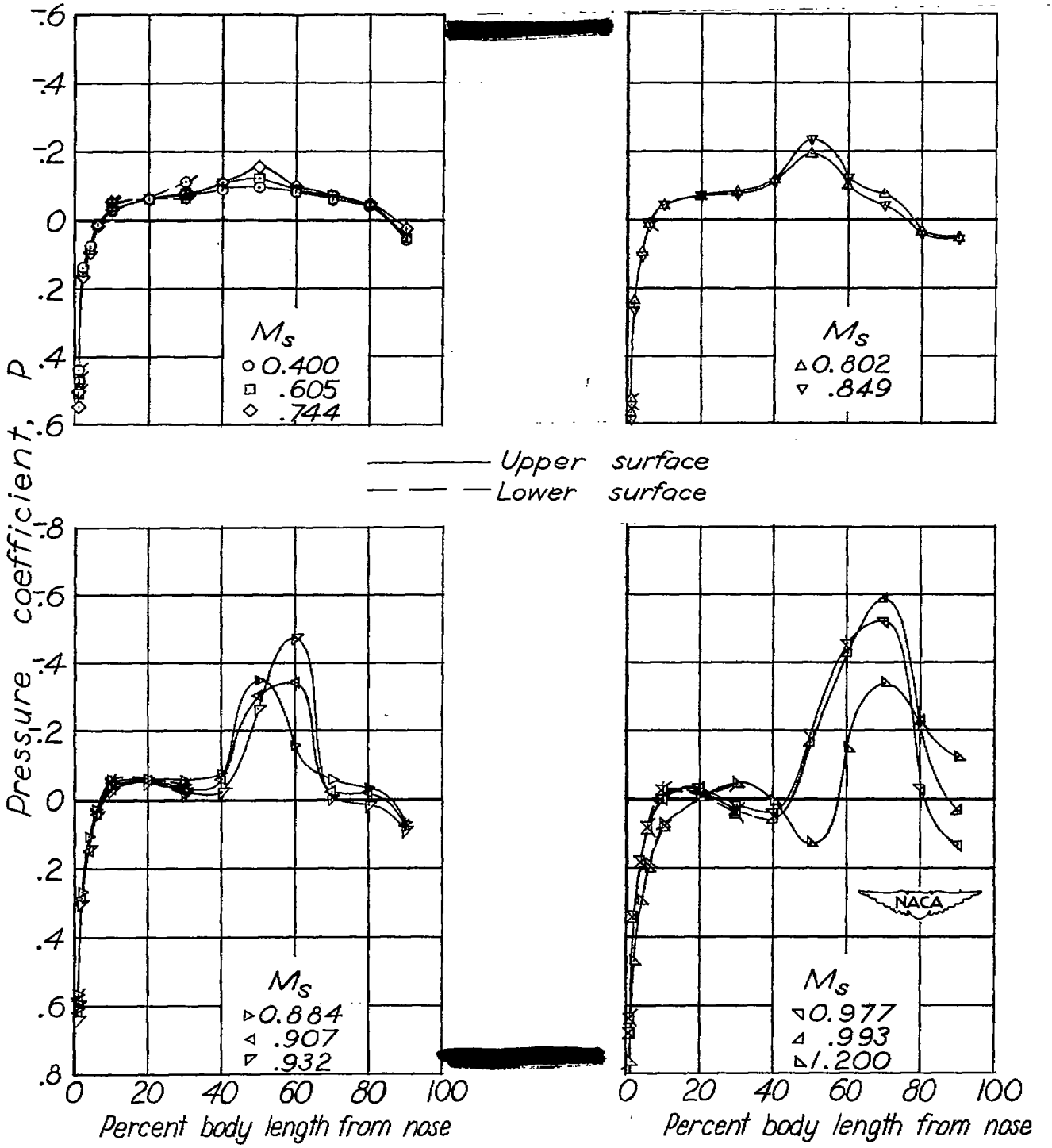

Figure 5. — Pressure distribution about fuselage. Complete model; $\alpha = 0°$. (The plain symbols refer to the upper surface and the flagged symbols refer to the lower surface.)

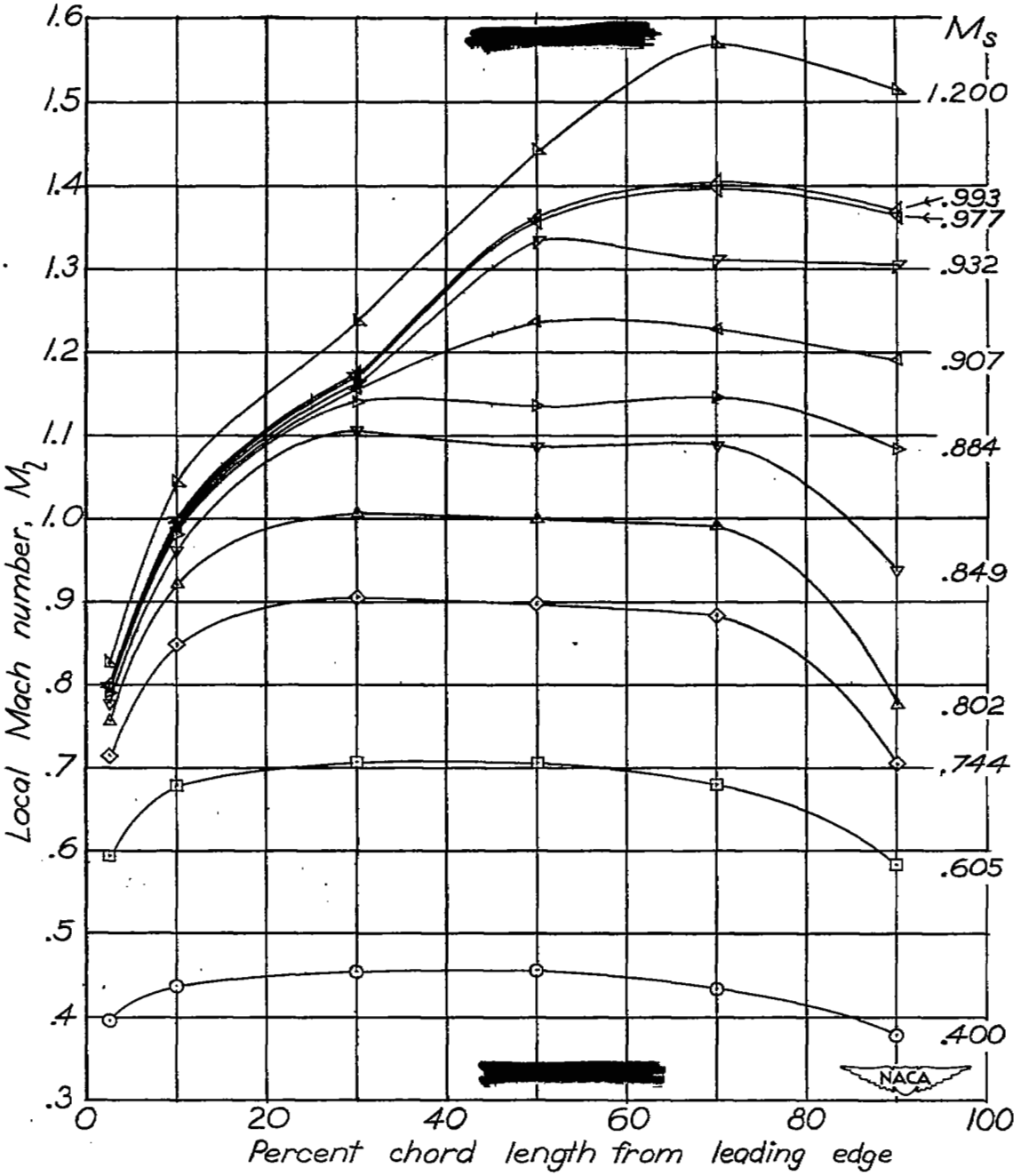

Figure. 6. — Chordwise Mach number distribution over wing. Complete model; $\alpha = 0°$.

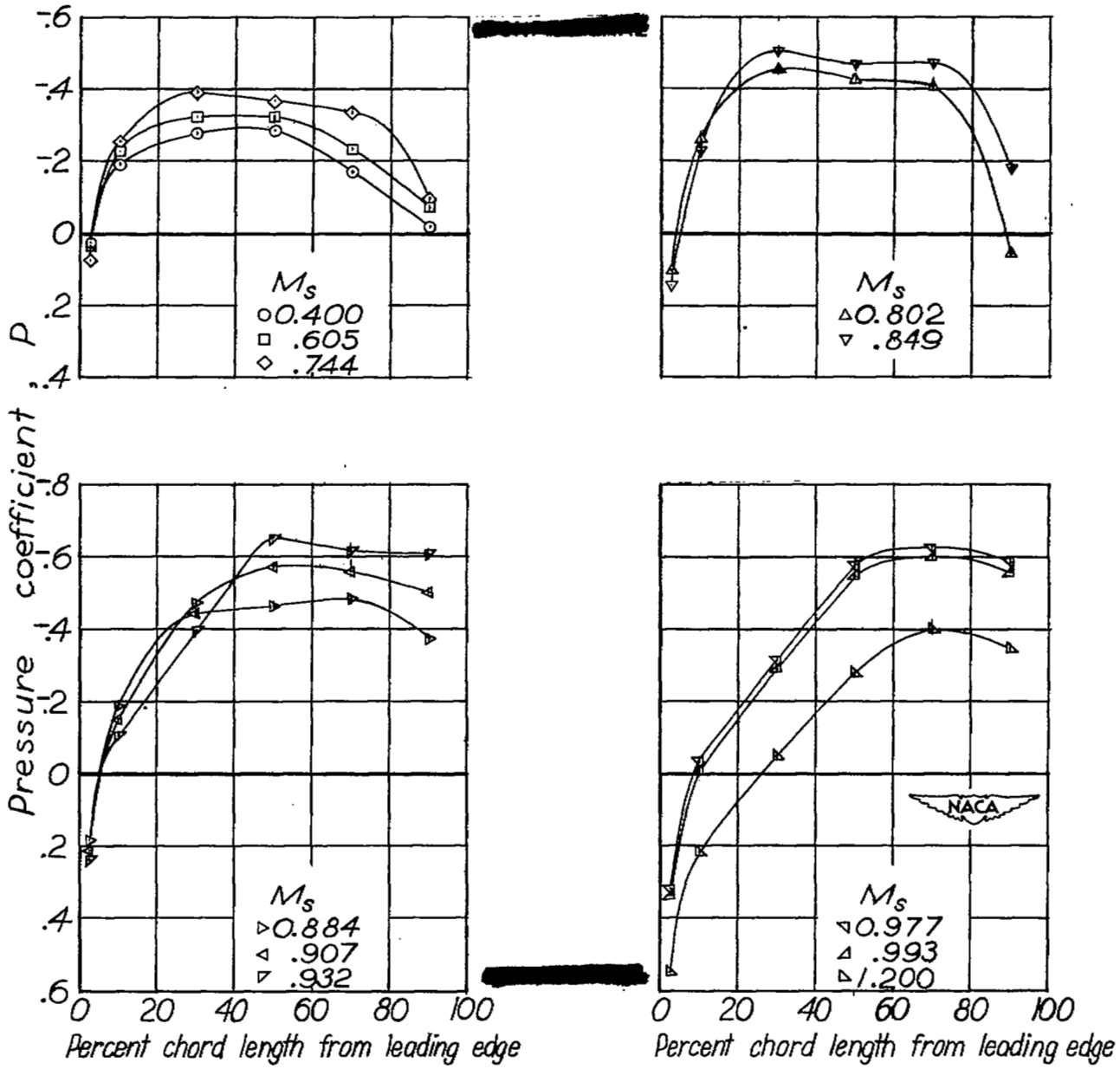

Figure 7. — Chordwise pressure distribution over wing. Complete model; $\alpha = 0°$.

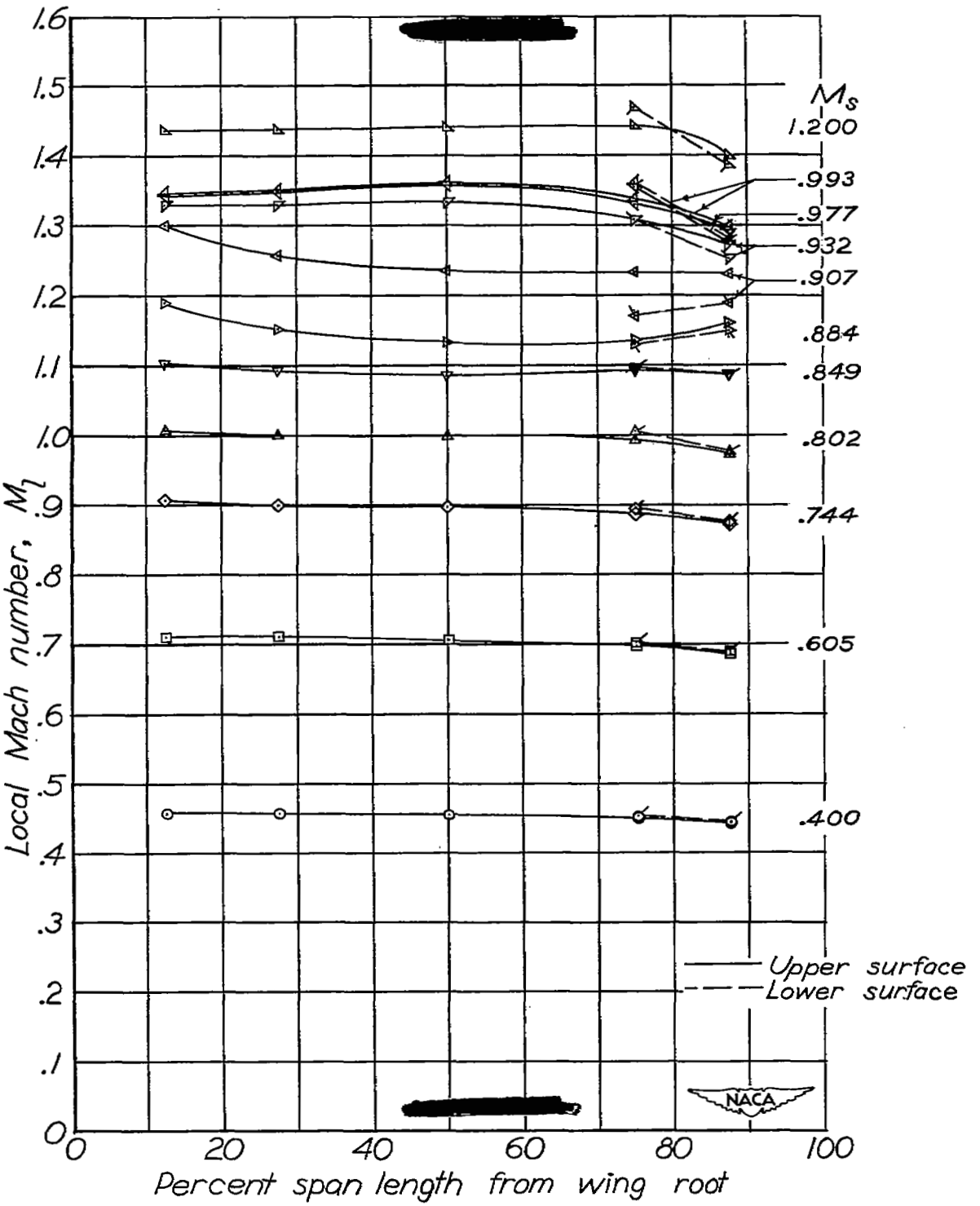

Figure 8.— Spanwise Mach number distribution about wing. Complete model; $\alpha = 0°$. (The plain symbols refer to the upper surface and the flagged symbols refer to the lower surface.)

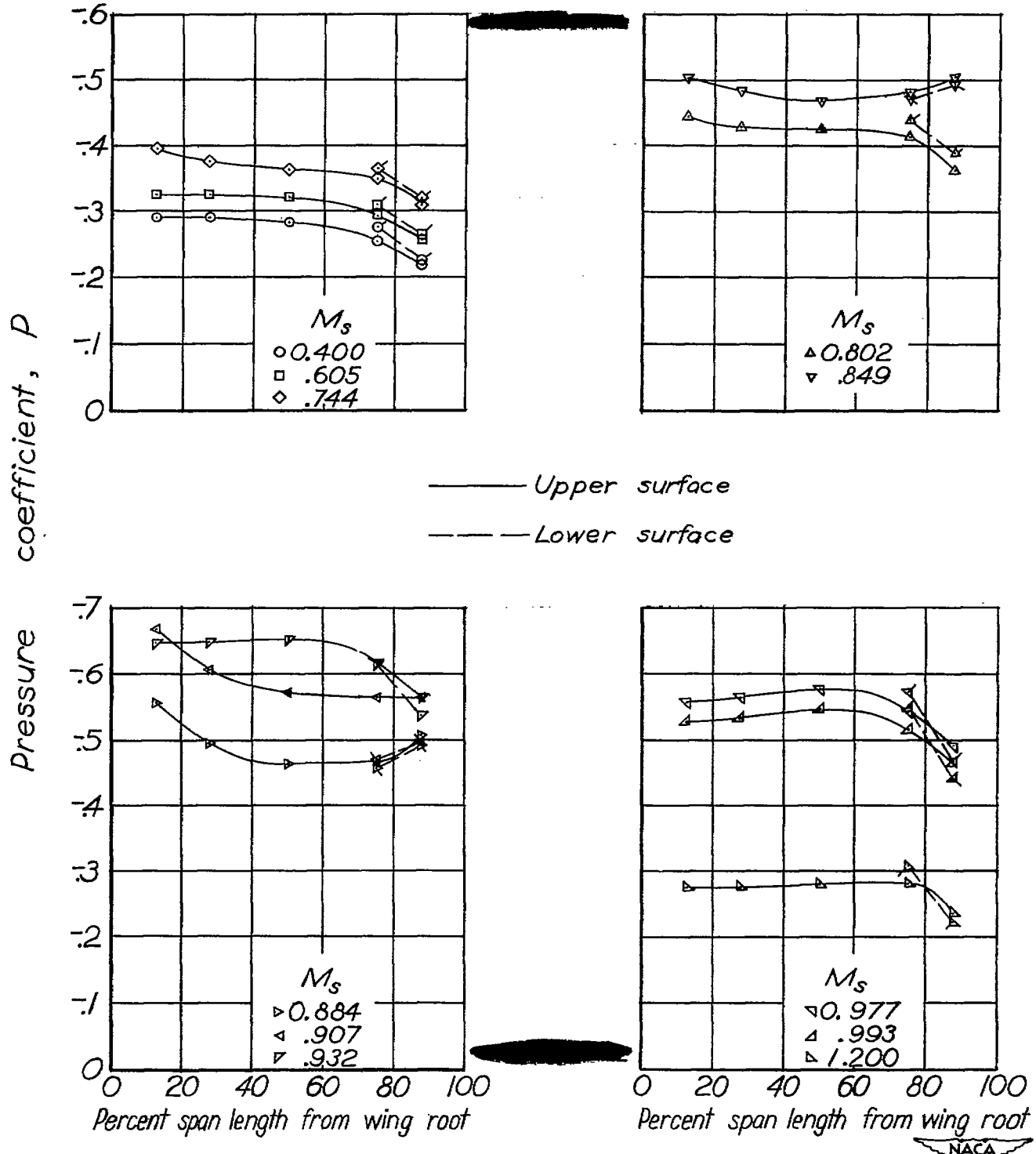

Figure 9. — Spanwise pressure distribution about wing. Complete model; $\alpha = 0°$. (The plain symbols refer to the upper surface and the flagged symbols refer to the lower surface.)

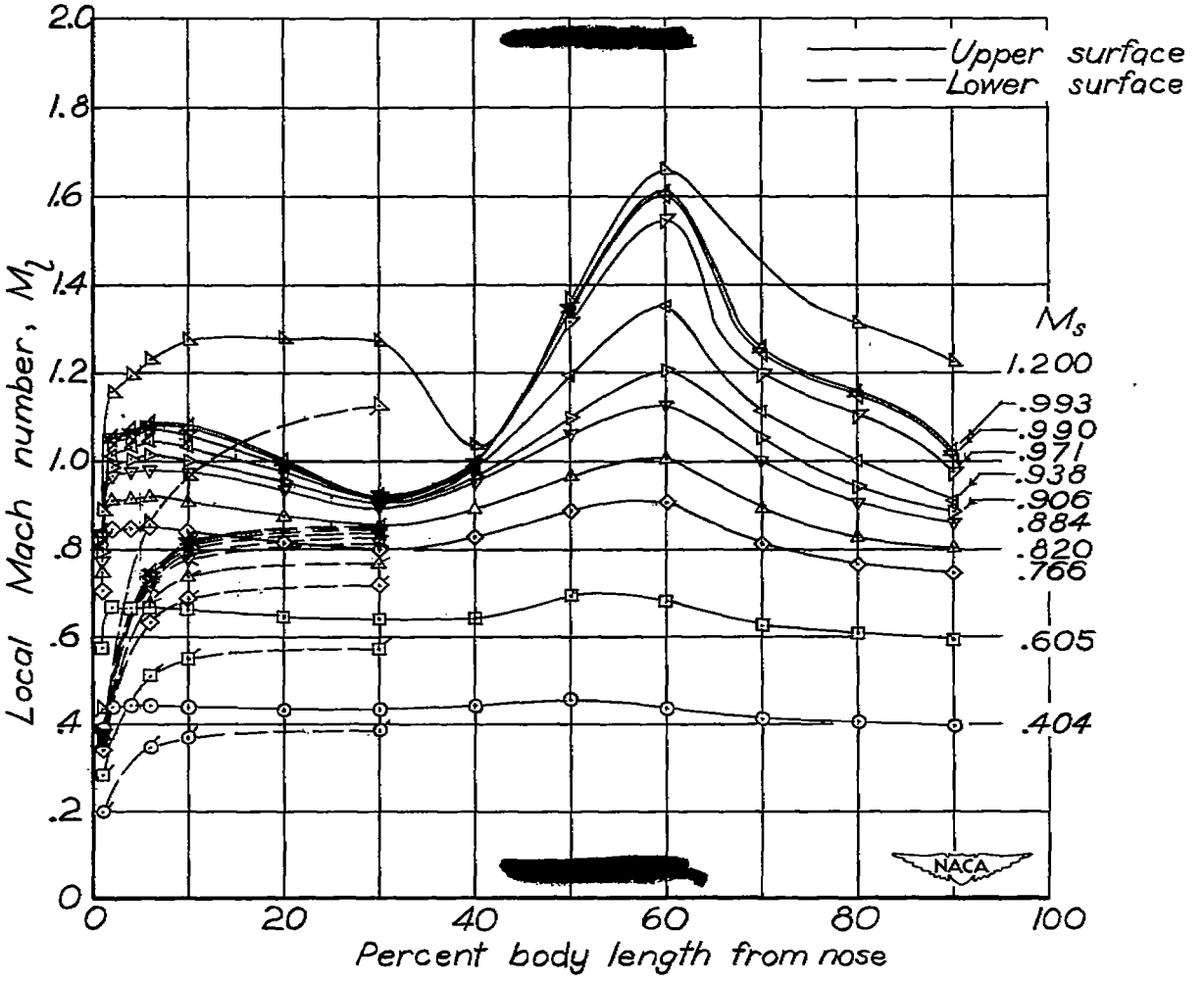

Figure 10. — Mach number distribution about fuselage. Complete model; $\alpha = 10°$. (The plain symbols refer to the upper surface and the flagged symbols refer to the lower surface.)

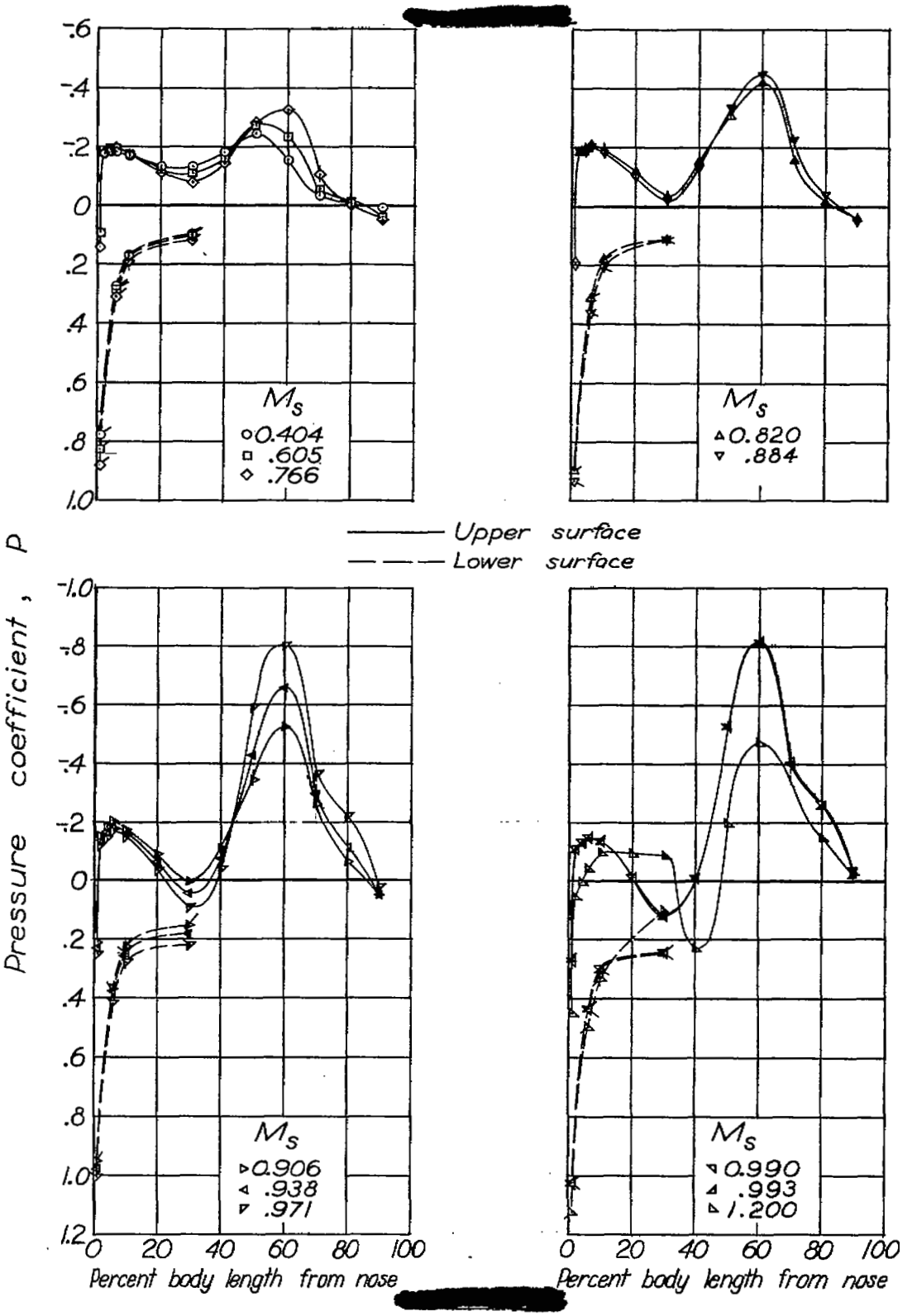

Figure 11.— Pressure distribution about fuselage. Complete model; $\alpha = 10°$. (The plain symbols refer to the upper surface and the flagged symbols refer to the lower surface.)

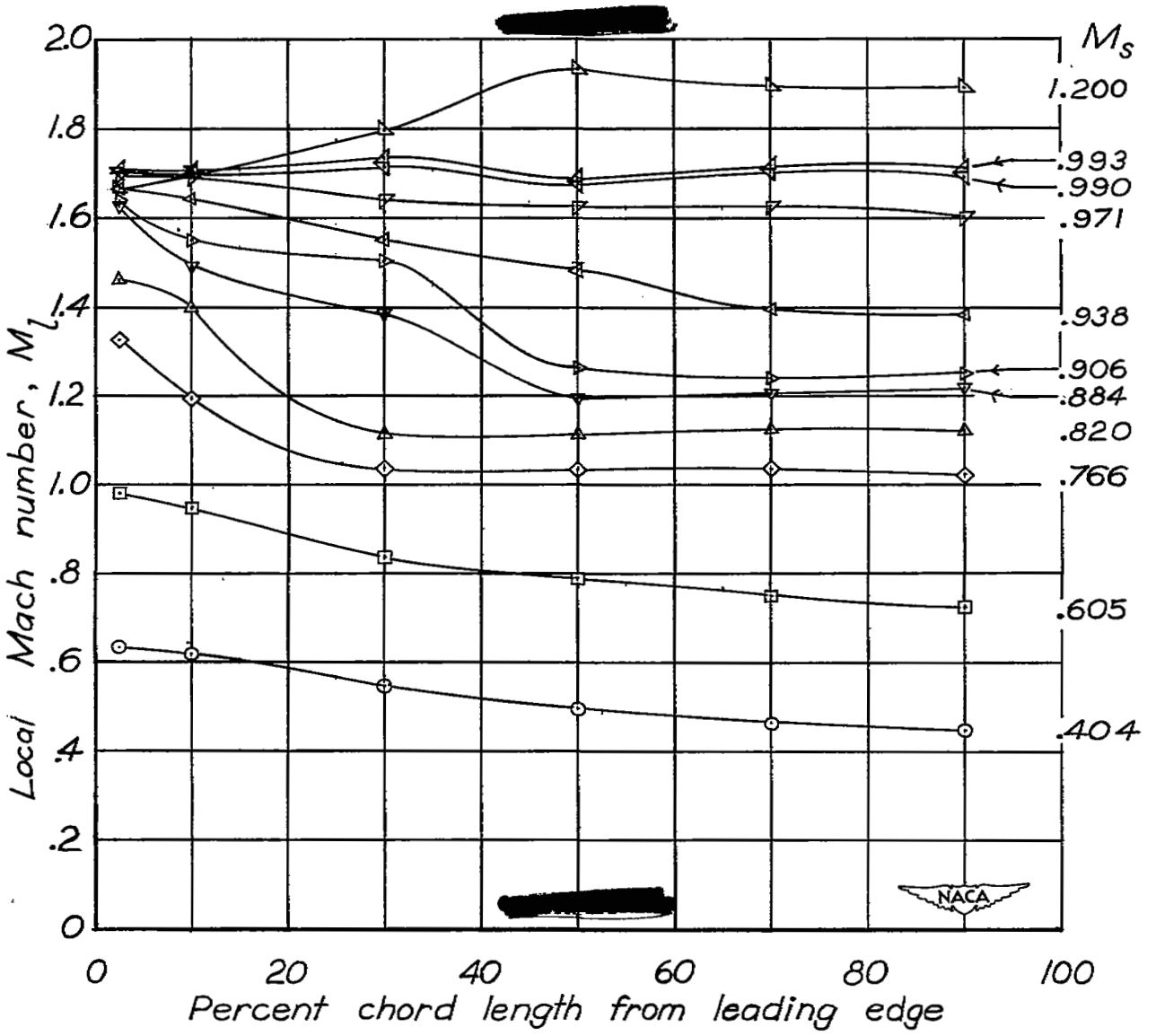

Figure 12.— Chordwise Mach number distribution over wing. Complete model; $\alpha = 10°$.

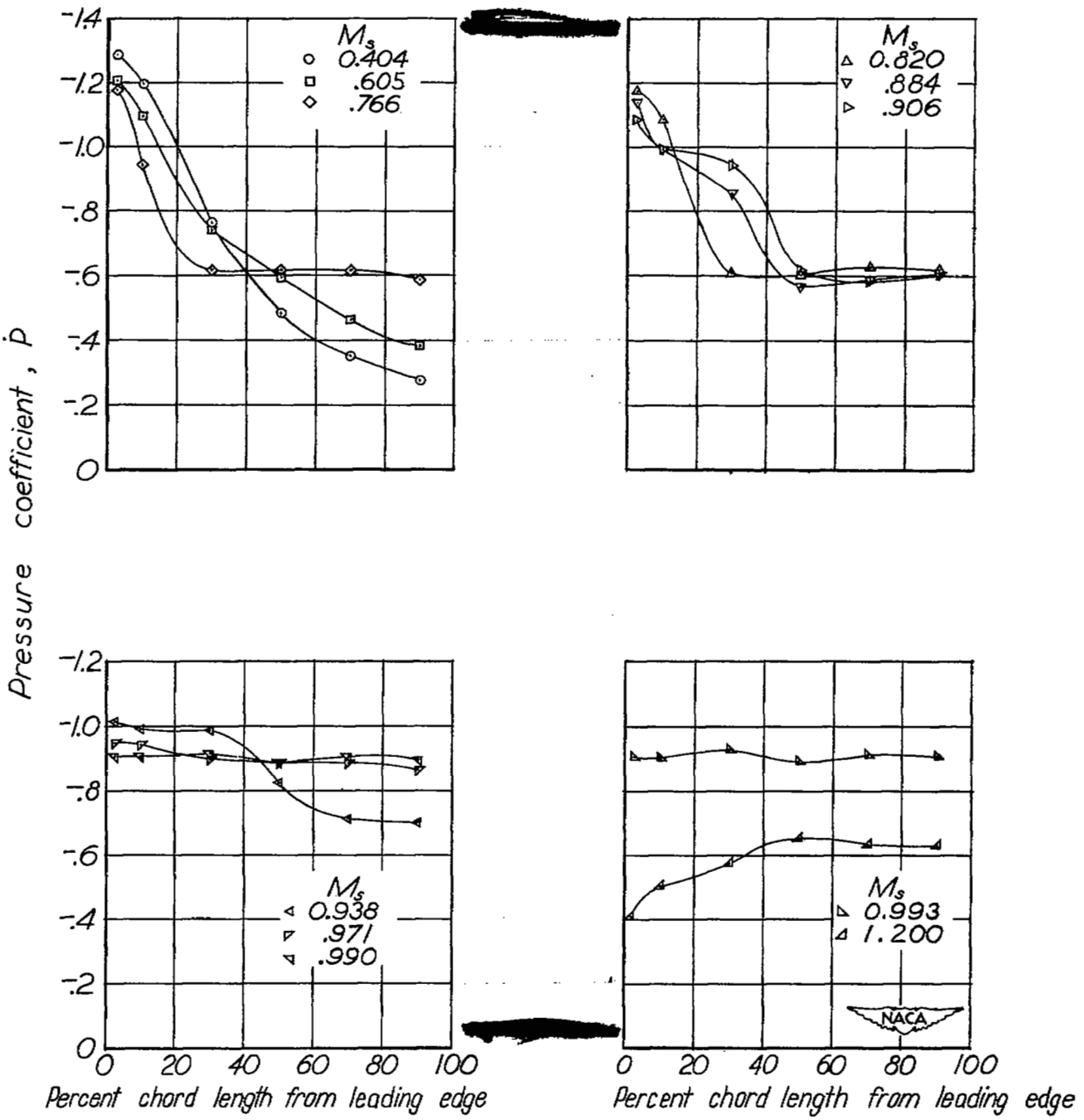

Figure 13. — Chordwise pressure distribution over wing. Complete model; $\alpha = 10°$.

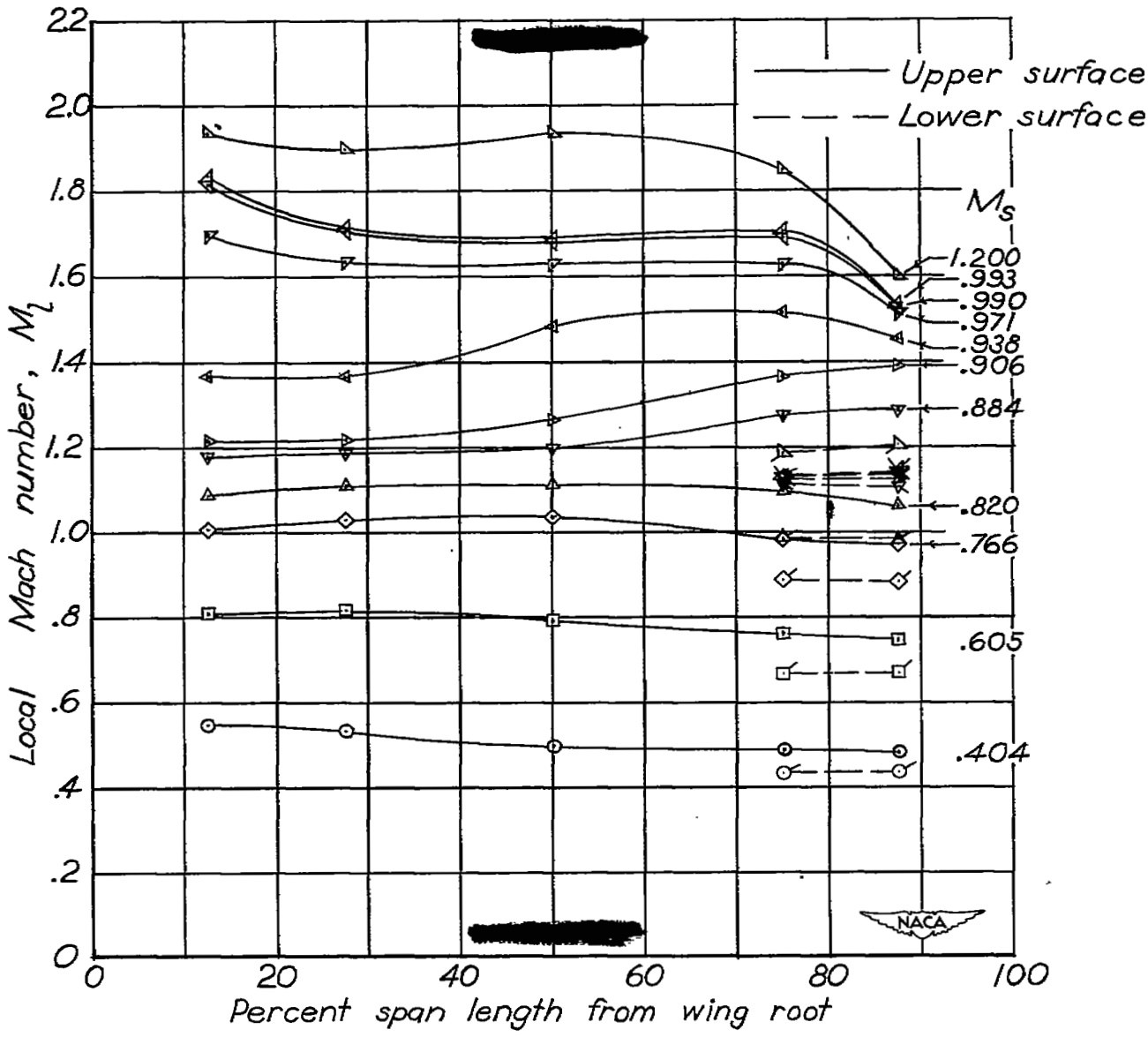

Figure 14.— Spanwise Mach number distribution about wing. Complete model; $\alpha = 10°$. (The plain symbols refer to the upper surface and the flagged symbols refer to the lower surface.)

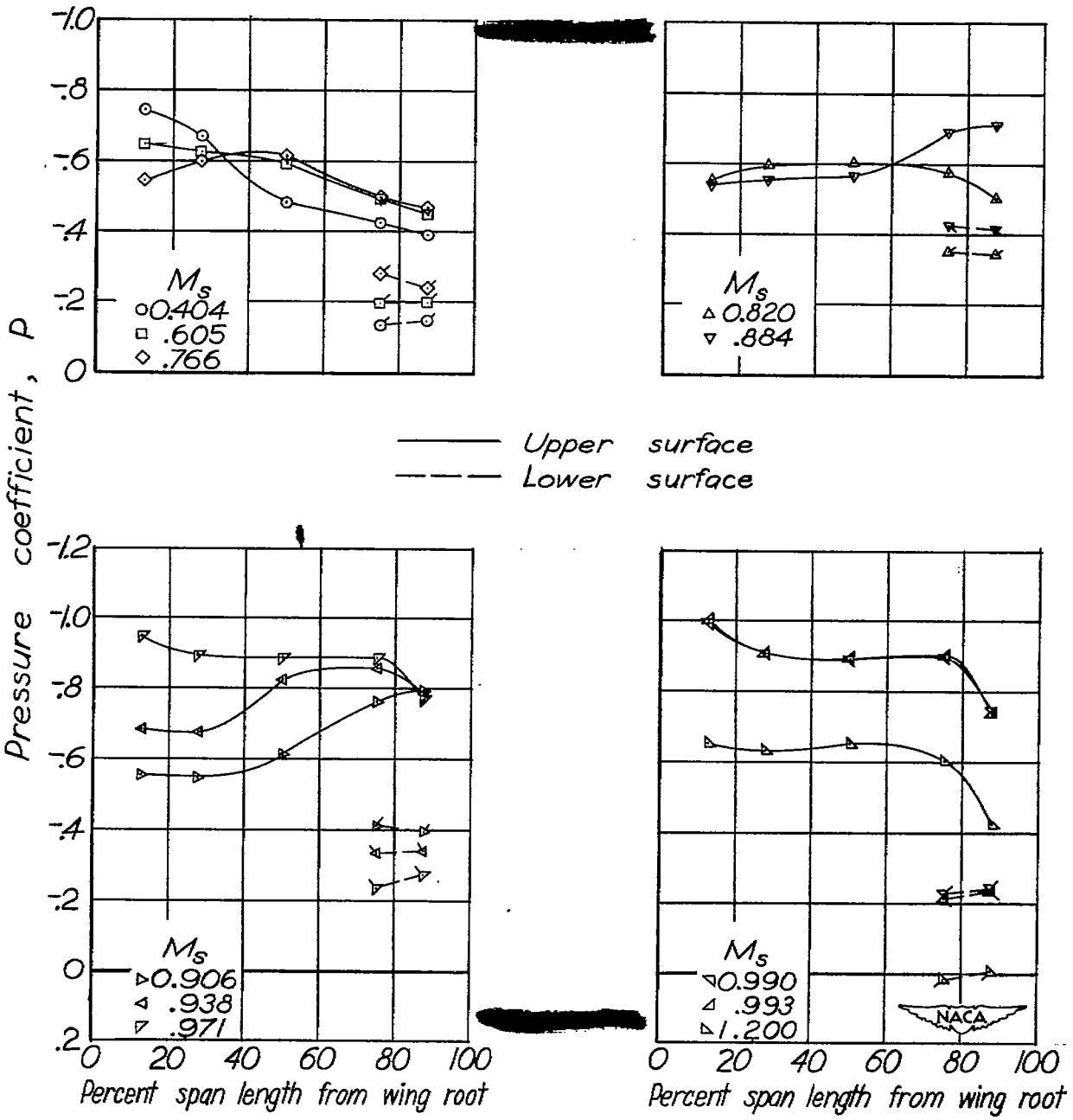

Figure 15.— Spanwise pressure distribution about wing. Complete model; $\alpha = 10°$. (The plain symbols refer to the upper surface and the flagged symbols refer to the lower surface.)

UNCLASSIFIED

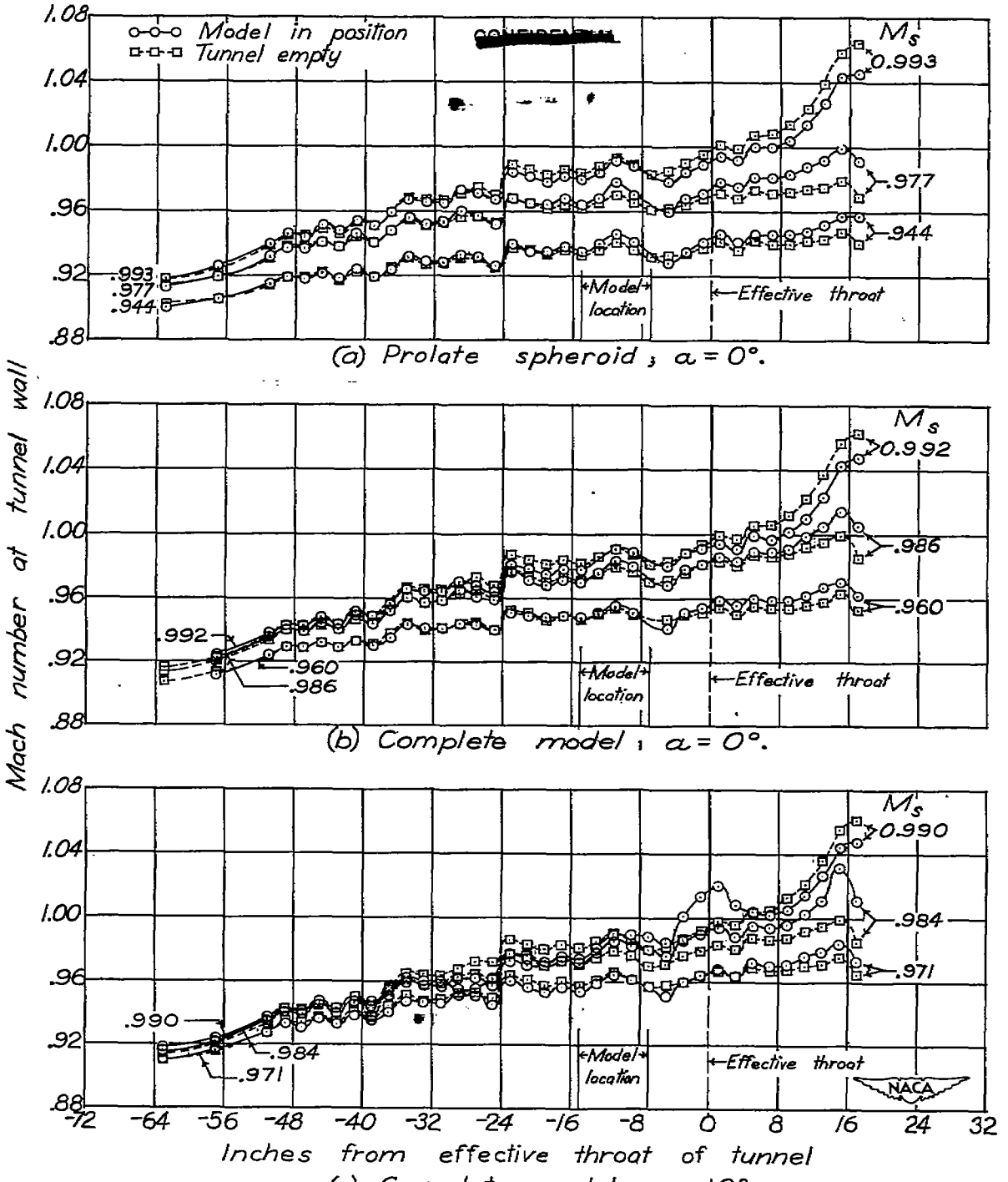

UNCLASSIFIED

Figure 16.— Comparison of local Mach numbers at tunnel wall with tunnel empty and with model in position. (The negative scale indicates locations upstream and the positive scale indicates locations downstream of effective throat of tunnel.)

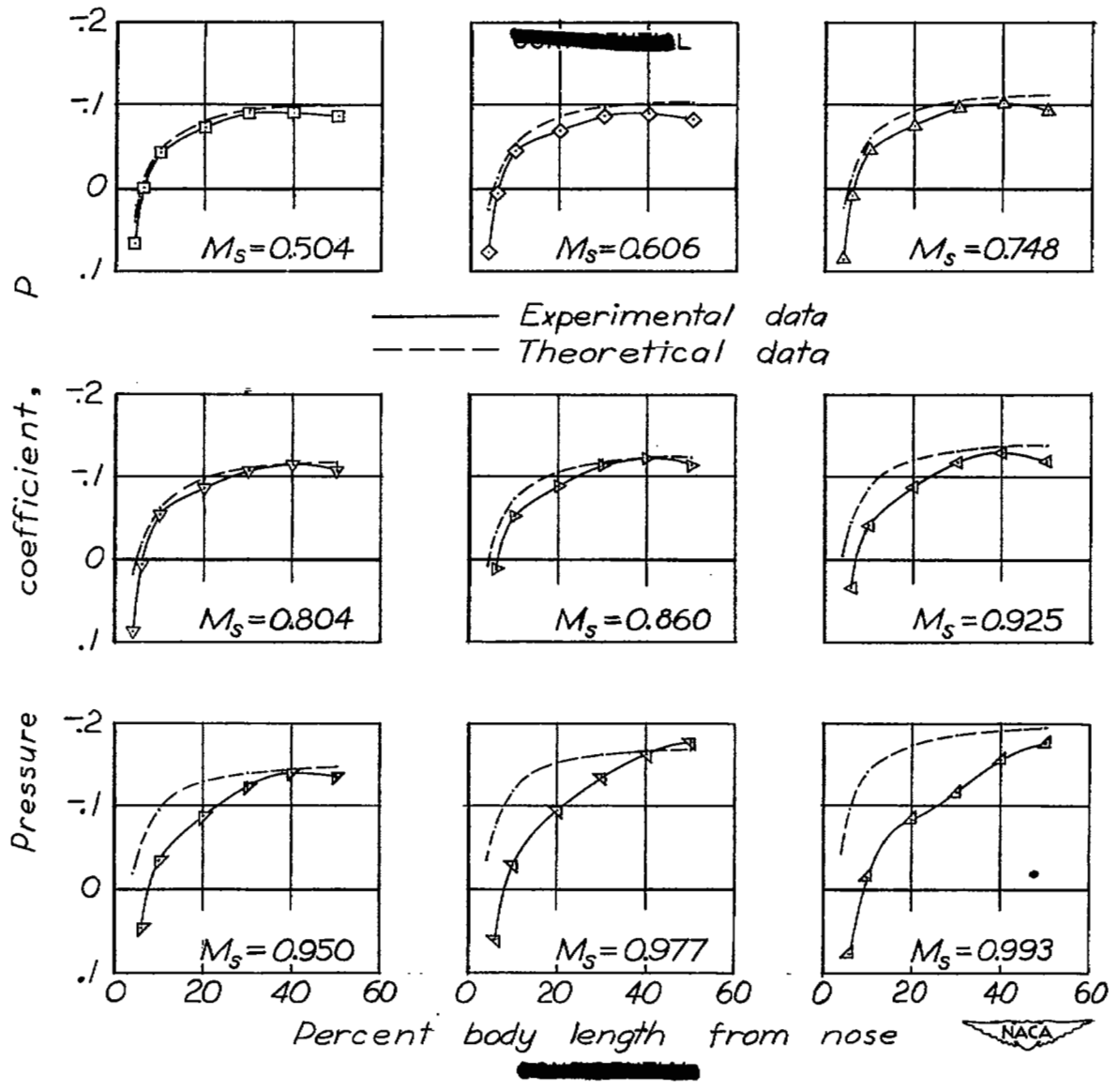

Figure 17. — Comparison of experimental and theoretical pressure distribution over a prolate spheroid with fineness ratio 6 for various stream Mach numbers. $\alpha = 0°$.